United Journal of Environment Sciences

Research Article

Treatment of Polyphenols and Aromatic Amines in Textile Industry Wastewaters by Cerium Dioxide -Titanium Dioxide

Sponza DT* and Oztekin R

Department of Environmental Engineering, Dokuz Eylül University, Turkey

Volume 1 Issue 1 - 2023
Received Date: 25 Jul 2023
Accepted Date: 12 Aug 2023
Published Date: 17 Aug 2023

2. Keywords

Cerium dioxide - titanium-dioxide; Nanocomposite; Polyaromatics; Polyphenols; Textile industry waste water

1. Abstract

In this study, CeO_2-TiO_2 nanocomposite was used for the photocatalytic degradation of pollutant parameters (Color, polyphenols (quercetin, fisetin, ellargic acid, carminic acid, luteolin, and curcumin) and polyaromatics [2,6-dimethylaniline (2,6-DMA), 2-aminoanisole (MOA), 2,4-toluenediamine (TDA), 2-naphthylamine (NA), 4,40-thiobisbenzenamine (TOA), 3,3-dichlorobenzidine (DCB) and 3,30-dimethoxybenzidine (DMOB)]. 15% CeO_2 -TiO_2 nanocomposite shows the highest photodegradation yield of color under both UV and visible-light irradiation, with maximum photo-degradation rates of 99% and 98.5%, respectively, after 30 min irradiation time. The results show that the CeO_2/TiO_2 nanocomposite has a high photocatalytic activity to remove the pollutants from TI ww.

3. Introduction

As an important semiconductor material, TiO_2 has been widely used as the photocatalyst because of its chemical and biological inertness, high stability against photocorrosion, non-toxicity, low cost, and excellent degradation for organic pollutants [1,2]. However, practical applications of the TiO_2 are still quite limited, mainly due to the low quantum efficiency and the broad bandgap responding only to UV light [3]. In order to improve the photocatalytic properties of TiO_2, much effort has been made, including transitional metal ion or non metal element doping [4,5], co-deposition of metals [6] and dye sensitization[7].

Cerium oxide and CeO_2-containing materials have been studied as a good alternative for the oxidation catalysts and supports. It has been shown that, when associated with transition metal oxides and noble metals, cerium oxide promotesoxygen storage and release to enhance oxygen mobility, and forms surface and bulk vacancies to improve the catalyst redox properties of the system [8,9].

Among them, coupling TiO_2 with CeO_2 attracts much attention because of the special f and d electron orbital structure and the special properties of CeO_2 [9]. It has been found that the variable valences of Ce such as Ce^{+4} and Ce^{+3} make CeO_2 possesses the excellent characteristics in transferring electrons and enhance the light absorption capability in near UV or UV [10]. Meanwhile, doping with CeO_2 can double oxygen reserve and transfer capacity of the TiO_2 photocatalysis [11]. Introducing CeO_2 into the TiO_2 framework could effectively extend the visible light response of TiO_2 [12]. Many researchers have focused on preparing meso-structured CeO_2–TiO_2 with a large surface area and controllable pore size to improve its photocatalytic activity [12]. The large surface area would improve the absorption and mass-transfer of target pollutants [13].

In the present study, nano-cerium dioxide doped titanium-dioxide (CeO_2-TiO_2) nanocomposite was firstly used for the photocatalytic degradation of pollutant parameters (color, polyphenols, polyaromatics) from the textile industry wastewater (TI ww) treatment plant in Izmir, Turkey, at different operational conditions such as at increasing photocatalytic time (0, 10, 15, 20, 30, 60, 90 and 120 min), at different CeO_2 -TiO_2 mass ratios (1%, 3%, 5%, 10%, 15%, 16%, 25%, 30%, 50%), at the different amounts of CeO_2 (1, 3, 5, 8, 10, 15, 20 and 25 mg/l) under 130 W UV and 35 W sun lights irradiations, respectively. Color, polyphenols (quercetin, fisetin, ellargic acid, carminic acid, luteolin, and curcumin) and polyaromatics [2,6-dimethylaniline (2,6-DMA), 2-aminoanisole (MOA), 2,4-toluenediamine (TDA), 2-naphthylamine (NA), 4,40-thiobisbenzenamine (TOA), 3,3-dichlorobenzidine (DCB) and 3,30-dimethoxybenzidine (DMOB)] removal efficiencies were observed during photocatalytic experiments.

***Corresponding Author (s):** Delia Teresa Sponza, Department of Environmental Engineering, Engineering Faculty, Dokuz Eylül University, Tınaztepe Campus, 35160, Buca/ Izmir, Turkey, Tel: +90 232 412 11 79, Fax: + 90 232 453 11 43, E-mail: delya.sponza@deu.edu.tr*

Citation: Sponza DT, Treatment of Polyphenols and Aromatic Amines in Textile Industry Wastewaters by Cerium Dioxide -Titanium Dioxide. United Journal of Environment Sciences. 2023; V1(1): 1-7.

4. Materials and Methods

4.1. Raw Wastewater

The TI ww used in this study contains color (> 70 1/m), total phenol (> 233 mg/l), COD_{dis} (> 770 mg/l) and high BOD_5 (> 251 mg/l) concentrations with a BOD_5/COD_{dis} ratio of 0.39. The characterization of TI ww was shown in (**Table 1**) for minimum, medium and maximum values.

Table 1: Characterization values of TI ww (n=3, mean values ± SD).

Parameters	Values		
	Minimum	Medium	Maximum
pH	5.10 ± 0.18	5.65 ± 0.20	6.20 ± 0.22
DO (mg/l)	1.32 ± 0.05	1.43 ± 0.05	1.54 ± 0.05
ORP (mV)	86.00 ± 3.01	107.55 ± 3.76	129.10 ± 4.52
TSS (mg/l)	286.00 ± 10.01	360 ± 12.6	434.00 ± 15.20
TVSS (mg/l)	193.00 ± 6.8	242.10 ± 8.47	291.20 ± 10.2
COD_{total}(mg/l)	932.60 ± 32.62	1171.40 ± 41.00	1410.10 ± 49.40
$COD_{dissolved}$(mg/l)	771.30 ± 27.00	968.8 ± 33.91	1166.30 ± 40.82
TOC (mg/l)	463.30 ± 16.22	582.90 ± 20.40	702.40 ± 24.60
BOD_5 (mg/l)	252.60 ± 8.84	315.4 ± 11.04	378.20 ± 13.24
BOD_5/COD_{dis}	0.37 ± 0.02	0.39 ± 0.014	0.41 ± 0.02
Total N (mg/l)	25.70 ± 0.90	30.96 ± 1.08	36.22 ± 1.27
NH_4-N (mg/l)	1.87 ± 0.07	2.25 ± 0.08	2.63 ± 0.092
NO_3-N (mg/l)	8.10 ± 0.28	10.2 ± 0.36	12.20 ± 0.43
NO_2-N (mg/l)	0.14 ± 0.005	0.16 ± 0.006	0.18 ± 0.006
Total P (mg/l)	8.90 ± 0.31	11.05 ± 0.39	13.20 ± 0.46
PO_4-P (mg/l)	6.34 ± 0.22	8.03 ± 0.28	9.72 ± 0.34
SO_4^{-2} (mg/l)	1250.10 ± 43.80	1560.8 ± 54.63	1871.40 ± 65.50
Color (m^{-1})	71.80 ± 2.51	89.05 ± 3.12	106.30 ± 3.72
Total phenol (mg/l)	234.00 ± 8.19	702.00 ± 24.57	936.00 ± 32.76
TAAs (mg benzidine /l)	1790.20 ± 62.66	3580.14 ± 125.31	5370.10 ± 188.00

4.2. Operational Conditions

The operational conditions were summarized in (**Table 2**). Time (0, 10, 15, 20, 30, 60, 90 and 120 min), at different CeO_2-TiO_2 mass ratios (1%, 3%, 5%, 10%, 15%, 16%, 25%, 30%, 50%), at the different amounts of CeO_2 (1, 3, 5, 8, 10, 15, 20 and 25 mg/l) under 130 W UV and 35 W sun lights irradiations, respectively. Color, polyphenols (quercetin, fisetin, ellargic acid, carminic acid, luteolin, and curcumin) and polyaromatics [2,6-dimethylaniline (2,6-DMA), 2-aminoanisole (MOA), 2,4-toluenediamine (TDA), 2-naphthylamine (NA), 4,40-thiobisbenzenamine (TOA), 3,3-dichlorobenzidine (DCB) and 3,30-dimethoxybenzidine (DMOB)] removal efficiencies were observed during photocatalytic experiments.

4.3. Analytical Methods

pH, T(°C), ORP (mV), TSS, TVSS, DO, BOD_5, COD_{total}, $COD_{dissolved}$, and TOC were monitored following Standard Methods 2550, 2580, 2540 C, 2540 E, 5210 B, 5220 D, 5310, 5520 B, respectively [15]. Total-N, NH_4-N, NO_3-N, NO_2-N, Total-P, PO_4-P, total phenol and SO_4^{-2} were measured with cell test spectroquant kits (Merck, Germany) at a spectroquant NOVA 60 (Merck, Germany) spectrophotometer (2003). The characterization of TI ww was shown in **Table 1** for minimum, medium and maximum values.

Table 2: Operational conditions under 130 W UV and 35 W sun light irradiations

Parameters				
Time (min)	CeO_2-TiO_2 mass ratios (%)	CeO_2 (mg/L)	polyphenols	Polyaromatics
0	1%	1	quercetin	2,6-dimethylaniline (2,6-DMA)
10	3%	3	fisetin	2-aminoanisole (MOA)
15	5%	5	ellargic acid	2,4-toluenediamine (TDA)
20	10%	8	carminic acid	2-naphthylamine (NA)
30	15%	10	luteolin	4,40-thiobisbenzenamine (TOA)
60	16%	15	curcumin	3,3-dichlorobenzidine (DCB)
90	25%	20		3,30-dimethoxybenzidine (DMOB)
120	30%	25		
	50%			

Gas chromatography/mass spectrometry (GC/MS) was used for the identification, gas chromatography nitrogen phosphorous detection (GC-NPD) for the quantification and gas chromatography flame ionization detection (GC-FID) for the determination of purity. The base peak of DCB, N-acetyl-DCB and N,N'-diacetyl-DCB was 252 m/z. The other main peaks were 294 m/z for N-acetyl-DCB, and 294 and 336 m/z for N,N'-diacetyl-DCB.

Polyphenols measurement was performed following the Standard Methods 5520 B [15] with a gas chromatography-mass spectrometry (GC-MS) (Hewlett-Packard 6980/HP5973MSD). Mass spectra were recorded using aVGTS 250 spectrometer equipped with a capillary SE 52 column (0.25 mm ID, 25 m) at 220°C with an isothermal program for 10 min. The total phenol was monitored as follows: 40 mL of TI ww was acidified to pH=2.0 by the addition of concentrated HCl. Phenols were then extracted with ethyl acetate. The organic phase was concentrated at 40°C to about 1 mL and silylized by the addition of N,O-bis(trimethylsilyl)acetamide (BSA). The resulting trimethylsilyl derivatives were analysed by GC-MS (Hewlett-Packard 6980/HP5973MSD). Polyphenols such as quercetin, fisetin, ellargic acid, carminic acid, luteolin, curcumin and polyaromatics such as 2,6-DMA, MOA, TDA, NA, TOA, DCB and DMOB were determined GC-MS (Hewlett-Packard 6980/HP5973MSD).

4.4. Preparation of Nano CeO_2 doped TiO_2 Nanocomposite under Laboratory Conditions

0.3 g of cerium nitrate ($Ce(NO_3)_3.6H_2O$, 98.5%, Daejung chemicals) was dispersed in 20 ml ethanol and a separate solution of titanium butoxide (97%, Sigma-Aldrich) in a mixture of ethanol:deionized (DI) water (20 ml/10 ml) was prepared. Afterwards, both the solutions were mixed and pH of 10 was maintained by the dropwise addition of ammonia solution (NH_3, 98%,

Daejung chemicals). The entire reaction solution was transferred into the teflon-beaker and sealed into a stainless steel autoclave and kept at 120°C for 48 h. After completion of the reaction, the autoclave was cooled at room temperature and the product was filtered, washed thoroughly with DI water, and dried overnight at 80°C. The as-synthesized material was calcined at 450°C with the ramp rate of 5°C/min.

5. Results and Discussion

5.1. Polyphenols in TI ww

The dyes in the textile industry is the main source of the color. The dyes used to color textiles are flavonoid compounds carotenoids, hydroxyketones, anthraquinones, naphthoquinones, flavones, flavonols, flavononones, indigoids and related compounds. Polyphenolic compounds that are expected to be found in the textile dyes are ellagic acid (simple phenolic acid); catechin, rutin, myricetin, luteolin, kaempferol, apigenin, morin, fisetin (flavonoids); curcumin (curcuminoid), carminic acid, purpurin and alizarin (having a core anthraquione structure). Among these polyphenols; quercetin, fisetin, ellagic acid, carminic acid, luteolin and curcumin concentrations were monitored as color polyphenols in TI ww.

At initial, color exhibits the maximum absorption wavelength at λ = 620 nm after 20 min photodegradation at 130 W UV using 15 mg/l CeO_2-TiO_2 nanocomposite with CeO_2 ratio of 15% (Figure 1). The maximum absorption wavelength was 560 nm with only 15 mg/l CeO_2 concentration while the maximum absorption wavelengths were 560 and 580 nm at 15 mg/l pure nano-TiO_2 and pure nano-CeO_2. The absorbance intensity of color gradually decreases with the increase of exposed time from 20 to 30 min, indicating the drastic decrease in the concentration of color originating from dyes in TI ww. The absorption wavelength λ decreased to 110 nm after 30 min for 15 mg/l CeO_2-TiO_2 nanocomposite with CeO_2 ratio of 15% while the adsorption wavelenthgs decreased to around 300 nm in both commercial nanoparticles (**Figure 1**). A reasonably high degradation rate of 99.3% of color within 30 min is detected over the surface of CeO_2–TiO_2 nanocomposite catalyst whereas, very low degradation rates (6% and 23%) is obtained when TI ww degradation takes place over the surface of commercial CeO_2 and TiO_2 catalysts under 130 W UV light illumination. The high color removal efficiency observed in this photocatalytic process is due to the fact that azo bond cleavage is easier in color giving polyphenols.

The maximum polyphenol yields were obtained after 30 min irradiation time under UV (**see Figure 2**). The maximum photooxidation yields for quercetin, fisetin and ellagic acid polyphenols were high (99%; 98% and 97%, respectively) while the yields for carminic acid, luteolin and curcumin polyphenols were sligthly low (88%, 82% and 80%, respectively). The electron orbital structure and the special properties of CeO_2 has been found that the variable valences of Ce such as Ce^{+4} and Ce^{+3} make CeO_2 possesses the excellent characteristics in transfer- ring electrons and enhance the light absorption capability in near ultraviolet or ultraviolet (Li et al. 2013). Meanwhile, doping with CeO_2 can double oxygen reserve and transfer capacity of the TiO_2 photocatalysis (Li et al. 2013). Based on the catalytic mechanism, the increasing O_2 adsorbed on the surface of particle can easily capture electron, which prohibits the undesirable recombination of electron-hole pair and greatly improves the catalytic oxidation activity.

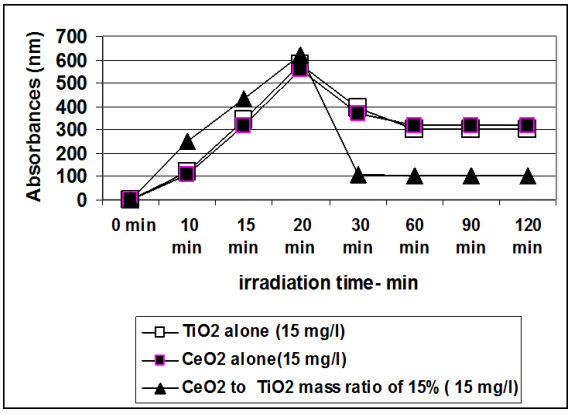

Figure 1: Absorbances of color versus produced nanocomposite and commercial nanoparticules under 130 W UVirradiation.

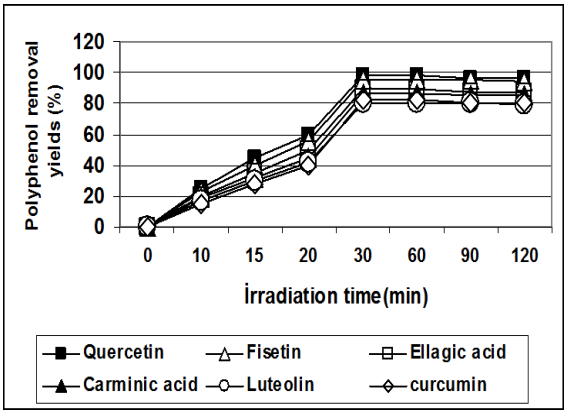

Figure 2: Removals of polyphenols via photooxidation using 15 mg/l CeO2 doped TiO_2 with a CeO_2 mass ratio of 15% under 130 W UV and at a pH=6.2

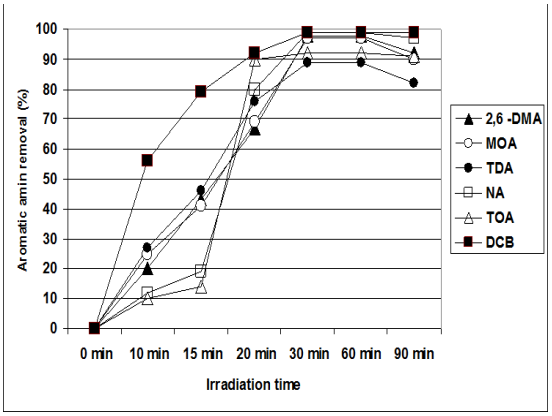

Figure 3: UV-vis absorbances of individual aromatic amines after photo degradation at 130 W UV power using 15 mg/l CeO_2 doped TiO_2 with a CeO_2 mass ratio of 15% at pH=6.2 at a temperature of 21°C.

5.2. Aromatic Amines in TIww

(Figure 3) shows the UV–Vis absorbance of individual aromatic amines with the exposed time of 0–120 min. After 20 min photooxidation the aromatic amines namely 2,6-DMA, MOA, TDA, NA, TOA, DCB and DMOB exhibited the maximum absorption wavelength at 515, 520, 580, 600, 540, 590 and 592 nm, respectively. The absorbance intensity of these aromatic amines decreased to 94, 95, 98, 90 and 88 nm with the increase of exposed time from 0 to 30 min, indicating the drastic decrease in the concentration of aromatic amines. A reasonably high degradation rate by 89-99% of aforementioned aromatic amines within 30 min are detected over the surface of CeO ₂TiO ₂nanocomposite catalyst whereas, low photodegradation rates (1, 3, 6, 8 and 10%) are obtained when aromatic amine photodegradation takes place over the surface commercial TiO_2 and CeO_2 catalysts under visible light illumination.

5.3. Aromatic Amine Metabolites

The formation of possible intermediates of 2,6-DMA, MOA, TDA, NA, TOA and DCB aromatic amines is illustrated in (**Table 3).** The intermediates of aromatic amines clearly reveal that the multiple fragmentation of aromatic amine macromolecule can lead the complete mineralization with the ending products of CO_2 and H_2O. DCB metabolites are N-acetyl-DCB and N,N'-diacetyl-DCB while N-phenylacetamide (acetanilide, NPA) and N-acetylated metabolites such as 5-OH-2-NA, 7-OH-2-NA and 8-OH-2-NA were detected as NA metabolites. From 350 mg/l DCB 200 mg/l N-acetyl-DCB and 90 mg/l N,N'-diacetyl-DCB produced. 2000 mg/l 2,6-DMA metabolized principally to 670 mg/l 4-hydroxy-2,6-dimethylaniline (4-HDMA), to 450 mg/l 2-amino- 3-methylbenzoic acid (2-AMBA), to 100 mg/l 2,6-dimethylnitrosobenzene and to 34 mg/l 3,5-dimethyl-4-imino-quinone during 130 W UV irradiation within 30 min photooxidation at 21ºC at 15 mg/l CeO_2 doped TiO_2, respectively. 250 mg/l MOA was converted to 80 mg/l cis-l,2-dihydroxy-3-methoxycyclohexa-3,5-diene (anisole-2,3-dihydrodiol), to 60 mg/l 2-methoxyphenol, to 20 mg/l catechol, and to trace amounts of phenol (3 mg/l) after 30 min photo-degradation at 21ºC with 15 mg/l CeO_2 doped TiO_2, respectively. 360 mg/l TDA metabolites were 40 mg/l 4-acetylamino-2-aminotoluene, 80 mg/l 2,4-diacetylaminotoluene, their phenolic derivatives (40 mg/l 4-acetylamino-2-aminobenzoic acid, and 10 mg/l 2,4-diacetylaminobenzoic acid) after 30 min irradiation times at 130 W UV power. 300 mg/l TOA metabolites are 20 mg/l benzidine, 120 mg/l mono-acethyl benzidine, 30 mg/l acethyl benzidine, 25 mg/l Cl-1 and 20 mg/l ethane after 30 min photo-degradation at 21ºC with 15 mg/l nano CeO_2 doped TiO_2, respectively.

DCB metabolites such as N-acetyl-DCB, N,N'-diacetyl-DCB removal efficiencies were 96% and 95%, after 30 min irradiation time (**Table 4**). 2, 6-DMA metabolites such as 4-hydroxy-2,6-dimethylaniline, 2-amino-3-methylbenzoic acid, 2,6-dimethylnitrosobenzene, 3,5-dimethyl-4-imino quinone removal efficiencies were 94%, 97%, 93%, 95%, respectively after 30 min irradiation time (**Table 4**). MOA metabolites such as cis-1,2-dihydroxy-3-methoxycyclohexa-3,5-diene, 2-methoxyphenol, catechol, trace amount of phenol removal efficiencies were 96%, 95%, 93%, 91%, respectively, after 30 min irradiation time (Table 4). TDA metabolites such as 4-acetylamino-2-aminotoluene, 2,4-diacetylaminotoluene, 4-acetylamino-2-aminobenzoic acid, 2,4-diacetylaminobenzoic acid removal efficiencies were 86%, 84%, 81%, 83%, respectively, after 30 min irradiation time (**Table 4**). TOA metabolites such as benzidine, mono-acethyl benzidine, acethyl benzidine, C1-1, ethane removal efficiencies were 91%, 90%, 90%, 88%, 92%, respectively after 30 min irradiation time (**Table 4**)(**Figure 4**).

Table 3: Removal efficiencies ofpolyphenol metabolite after 10 min and 30 min irradiation with nano CeO2-TiO2 under 130 W UVpower

Polyphenol Metabolite name and Influent Conc. (mg/l)	After 10 min irradiation with… nano Ce_2O_2-TiO_2 under 130 W UV power Conc. (mg/l)	Removal Eff. (%) after 10 min	After 30 min irradiation with… nano Ce_2O_2-TiO_2 under 130 W UV power Conc. (mg/l)	Removal Eff. (%) after 30 min	Effluent remaining conc. (mg/l)
Quercetin metabolites					
Isorhamnetin 20 mg/l	15.6	22	0.4	98	0.4
Tamarixetin 46 mg/l	36.34	21	1.84	96	1.84
Fisetin metabolites					
3'-4'-catechol 40 mg/l	30	25	2.4	94	2.4
Ellagic acid metabolites					
3, 8-dihydroxy-6H dibenzopyran-6-one 43 mg/l	32.25	25	4.3	90	4.3
3-hydroxyurolithin 15 mg/l	12	20	1.05	93	1.05
7-hydroxy-3,4-benzocoumarin 10 mg/l	7.8	22	0.6	94	0.6
Carminic acid metabolites					
C-glucopyranosyl flauokermesic 30 mg/l	24.3	19	4.8	84	4.8
Glucopyranosyl-dioxoanthracene 20 mg/l	15.2	24	2.8	86	2.8
Luteolin metabolites					
3'-methylluteolin 20 mg/l	16.2	19	4	80	4
4'-methylisomer 18 mg/l	14.22	21	3.96	78	3.96
Curcumin metabolites					
Bisdemethoxycurcumin 34 mg/l	27.88	18	7.48	78	7.48
O-glucuronide 20 mg/l	16	20	5.2	74	5.2
Curcumin O-sulfate 8 mg/l	6.16	23	2.24	72	2.24

Table 4: Removal efficiencies of aromatic amines metabolite after 10 min and 30 min irradiation with nano CeO2-TiO2 under 130 W UVpower

Aromatic amine metabolite name and influent conc. (mg/l)	After 10 min irradiation with nano Ce_2O_2-TiO_2 under 130 W UV power conc. (mg/l)	Removal Eff. (%) after 10 min	After 30 min irradiation with nano Ce_2O_2-TiO_2 under 130 W UV power conc. (mg/l)	Removal Eff. (%) after 30 min	Effluent remaining conc. (mg/l)
DCB metabolites					
N-acetyl-DCB 200 mg/l	92	54	8	96	8
N,N'-diacetyl-DCB 90 mg/l	45	50	4.5	95	4.5
2, 6-DMA metabolites					
4-hydroxy-2,6-dimethyaniline 670 mg/l	549.4	18	40.2	94	40.2
2-amino-3-methylbenzoic acid 450 mg/l	369	18	13.5	97	13.5
2, 6-dimethyl-nitrosobenzene 100 mg/l	81	19	7	93	7
3, 5-dimethyl-4-iminoquinone 34	27.2	20	1.7	95	1.7
MOA metabolites					
cis-1, 2-dihydroxy-3-methoxycyclohexa-3,5-diene 80 mg/l	65.6	18	3.2	96	3.2
2-methoxyphenol 60 mg/l	48.6	19	3	95	3
Catechol 20 mg/l	16.2	19	1.4	93	1.4
Trace amounts of phenol 3 mg/l	2.49	17	0.27	91	0.27
TDA metabolites					
4-acetylamino-2-aminotoluene 40 mg/l	29.6	26	5.6	86	5.6
2,4-diacetyl-aminotoluene 80 mg/l	60.8	24	12.8	84	12.8
4-acetylamino-2-aminobenzoic acid 40 mg/l	31.2	22	7.6	81	7.6
2,4-diacetylaminobenzoic acid 10 mg/l	7.8	22	1.7	83	1.7
TOA metabolites					
Benzidine 20 mg/l	18.2	9	1.8	91	1.8
Mono-acethyl benzidine 120 mg/l	110.4	8	12	90	12
Acethyl benzidine 30 mg/l	27.6	8	3	90	3
C1-1 25 mg/l	23.25	7	3	88	3
Ethane 20 mg/l	18.4	8	1.6	92	1.6
NA metabolites					
DMOB metabolites					

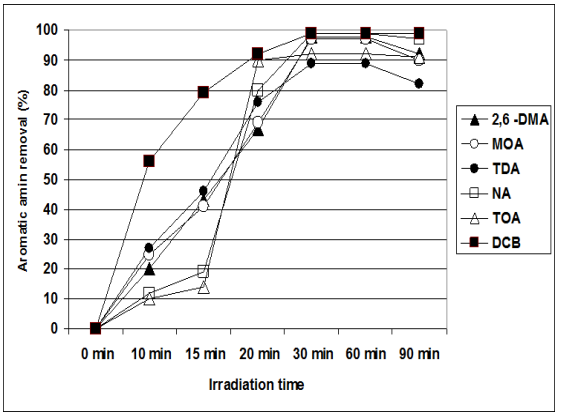

Figure 4: Photo oxidation yields of decomposed TI ww for aromatic amines under 130 W UV power, at 21°C with 15 mg/l CeO_2 doped TiO_2

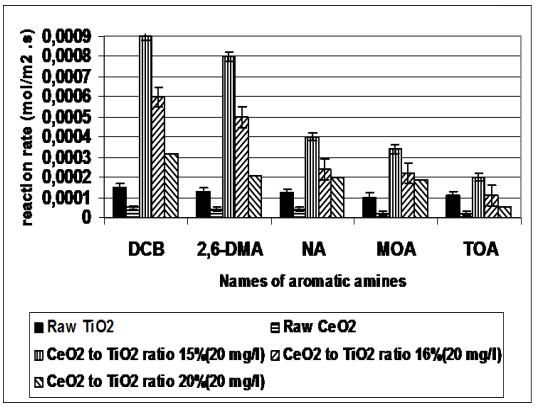

Figure 5: Aromatic amine reaction rates

6. Conclusions

The maximum photooxidation yields for quercetin, fisetin and ellagic acid polyphenols were high (99%, 98% and 97%, respectively) while the yields for carminic acid, luteolin and curcumin polyphenols were sligthly low (88%, 82% and 80%, respectively). The maximum yield was observed as 99% for DCB aromatic amine while the yields for MOA and NA were calculated as 98% and 97%, respectively after 30 min irradiation time at a power of 130 W UV. It is an economical and environmentally sustainable method to utilize sunlight as a natural source of energy to treat dye wastewater through photocatalytic process.

7. Acknowledgements

This research study was undertaken in the Environmental Microbiology Laboratury at Dokuz Eylül University Engineering Faculty Environmental Engineering Department, İzmir, Turkey. The authors would like to thank this body for providing financial support.

References

1. Linsebigler AL, Lu G, Yates JT. Photocatalysis on TiO2 surfaces: principles, mechanisms, and selected results. Chemical Reviews. 1995; 95(3): 735-758.

2. Asahi R, Morikawa T, Ohwaki T, Aoki K, Taga Y. Visible-light photocatalysis in nitrogen-doped titanium oxides. Science. 2001;293(5528): 269-271.

3. Zheng Y, Shi E, Chen Z, Li W, Hu X. Influence of solution concentration on the hydrothermal preparation of titania crystallites. Journal of Materials Chemistry. 2001; 11(5):1547-1551.

4. Yamashita H, Harada H, Misaka J, Takeushi M, Ikeue K, Anpo M. Degradation of propanol diluted in water under visible light irradiation using metal ionimplanted titanium dioxide photocatalysts. Journal of Photochemistry and Photobiology A: Chemistry. 2002; 148(1-3): 257-261.

5. Yu JC, Zhang L, Zheng Z, Zhao J. Synthesis and characterization of phosphated mesoporous titanium dioxide with high photocatalytic activity. Chemistry of Materials. 2003; 15(11): 2280-2286.

6. Wang W, Zhang J, Chen F, He D, Anpo M. Preparation and photocatalytic properties of Fe3+-doped Ag@TiO2 core–shell nanoparticles. Journal of Colloid and Interface Science. 2008; 323(1): 182-186.

7. Chen F, Zou W, Qu W,Zhang J. Photocatalytic performance of a visible light TiO2 photocatalyst prepared by a surface chemical modification process. Catalysis Communications. 2009; 10(11): 1510-1513.

8. Bhargava SK, Tardio J, Prasad J, Foger K, Akolekar DB, Grocatt SC. Wet oxidation and catalytic wet oxidation. Industrial & Engineering Chemistry Research. 2006; 45(4):1221-1258.

9. Massa P, Ivorra F, Haure P, Medina Cabello F, Fenoglio R. Catalytic wet air oxidation of phenol aqueous solutions by 1% Ru/CeO2–Al2O3 catalysts prepared by different methods. Catalysis Communications. 2007; 8(3): 424-428.

10. Pavasupree S, Suzuki Y, Pivsa-Art S, Yoshikawa S. Preparation and characterization of mesoporous TiO2–CeO2 nanopowders respond to visible wavelength. Journal of Solid State Chemistry. 2005; 178(1):128-134.

11. Morimo T, Dutta G, Waghmare UV, Baidya T, Hegde MS, Priolkar KR, Sarode PR. Origin of enhanced reducibility/oxygen storage capacity of Ce1−xTixO2 compared to CeO2 or TiO2. Chemistry of Materials. 2006; 18(14): 32493256.

12. Li G, Zhang D, Yu JC. Thermally stable ordered mesoporous CeO2/TiO2 visible-light photocatalysts. Physical Chemistry Chemical Physics. 2009; 11(19):3775-3782.

13. Li M, Zhang S, Lv L, Wang M, Zhang W, Pan B. A thermally stable mesoporous ZrO2–CeO2–TiO2 visible light Photocatalyst. Chemical Engineering Journal. 2013; 229:118-125.

14. Eaton AD, Clesceri LS, Rice EW, Greenberg AE, Franson MAH. Standard methods for the examination of water and wastewater. In M. A. H. Franson (Eds.), (21th ed.), Washington, DC: American Public Health Association (APHA), American Water Works Association (AWWA), Water Environment Federation (WEF). American Public Health Association 800 I Street, NW, 20001-3770, USA. 2005.

15. Ameen S, Akhtar MS, Seo HK, Shin HS. Solution-processed CeO2/TiO2 nanocomposite as potent visible light photocatalyst for the degradation of bromophenol dye. Chemical Engineering Journal. 2014; 247: 193-198.

16. Balavi H, Samadanian-Isfahani S, Mehrabani-Zeinabad M, Edrissi M. Preparation and optimization of CeO2 nanoparticles and its application in photocatalytic degradation of Reactive Orange 16 dye. Powder Technology. 2013; 249:549-555.

17. Besson M, Descorme C, Bernardi M, Gallezot P, Di Gregorio F, Grosjean N, et al. Supported noble metal catalysts in the catalytic wet air oxidation of industrial wastewaters and sewage sludges. Environmental Technology. 2010; 31(13): 1441-1447.

18. Chen XB, Mao SS. Titanium dioxide nanomaterials: Synthesis, properties, modifications, and applications. Chemical Reviews. 2007; 107(7): 2891-2959.

19. Esplugas S, Yue PL, Pervez MI. Degradation of 4-chlorophenol by photolytic oxidation. Water Research. 1994; 28(6): 1323-1328.

20. Jain R, Sikarwar S. Semiconductor-mediated photocatalyzed degradation of erythrosine dye from wastewater using TiO2 catalyst. Environmental Technology. 2010; 31(12):1403-1410.

21. Ji P, Tian B, Chen F, Zhang J. CeO2 mediated photocatalytic degradation studies of C.I. acid orange 7. Environmental Technology. 2012l 33(4): 467-472.

22. Liu B, Zhao X, Zhang N, Zhao Q, He X, Feng J. Photocatalytic mechanism of TiO2–CeO2 films prepared by magnetron sputtering under UV and visible light. Surface Science. 2005; 595(1-3): 203-211.

23. Liu H, Wang M, Wang Y, Liang Y, Cao W, Su Y. Ionic liquid-templated synthesis of mesoporous CeO2–TiO2 nanoparticles and their enhanced photocatalytic activities under UV or visible light. Journal of Photochemistry and Photobiology A: Chemistry. 2011; 223(2-3): 157-164.

24. Masten SJ, Davies SHR. The use of ozonation to degrade organic contaminants in wastewaters. Environmental Science & Technology. 1994; 28(4): 180A-185A.

25. Pirkarami A, Olya ME, Farshid SR. UV/Ni–TiO2 nanocatalyst for electrochemical removal of dyes considering operating costs. Water Resources and Industry. 2014; 5:9-20.

26. Pouretedal HR, Beigy H, Keshavarz MH. Bleaching of Congo red in the presence of ZnS nanoparticles, with dopant of Co2+ ion, as photocatalyst under UV and sunlight irradiations. Environmental Technology. 2010; 31(11): 1183-1190.

27. Riss A, Elser MJ, Bernardi J, Diwald O. Stability and photoelectronic properties of layered titanate nanostructures. Journal of the American Chemical Society 2009; 131(17):6198-6206.

28. Shao X, Lu W, Zhang R, Feng Pan F. Enhanced photocatalytic activity of TiO2-C hybrid aerogels for methylene blue degradation. Scientific Reports. 2013; 3: 3018, doi: 10.1038/srep03018, 1-9.

29. Subramonian W, Wu TY. Effect of enhancers and inhibitors onphotocatalytic sunlight treatment of Methylene Blue. Water, Air, & Soil Pollution. 2014; 225(5): 1922-1937.

30. Vohraa MS, Selimuzzaman SM, Al-Suwaiyan MS. NH4+-NH3 removal from simulated wastewater using UV, TiO2 photocatalysis: Effect of co-pollutants and pH. Environmental Technology. 2010; 31(6): 641-654.

31. Yang H, Zhang K, Shi R. Sol-gel synthesis and photocatalytic activity of CeO2/TiO2 nanocomposites. Journal of the American Ceramic Society. 2007; 90(5):1370-1374.

32. Zhao B, Shi B, Zhang X, Cao X, Zhang Y. Catalytic wet hydrogen peroxide oxidation of H-acid in aqueous solution with, TiO2–CeO2 and Fe/TiO2–CeO2 catalysts. Desalination. 2011; 268(1-3): 55-59.

33. Zubkov T, Stahl D, Thompson TL, Panayotov D, Diwald O, Yates JJT. Ultraviolet light-induced hydrophilicity effect onTiO2(110)(1×1). Dominant role of the photooxidation of adsorbed hydrocarbons causing wetting by water droplets. Journal of Physical Chemistry B. 2005; 109(32): 15454-15462.